Proceedings of the 39th IEEE
Conference on Decision and Control
Sydney, Australia • December, 2000

Polygonal approximation of uncertain height fields for outdoor navigation

Mauro Di Marco, Domenico Prattichizzo, Antonio Vicino

Dipartimento di Ingegneria dell'Informazione, Università di Siena
Via Roma, 56 - 53100 Siena, Italia

Abstract

Exploring unstructured and unknown environments is one of the most important tasks of mobile robotics. Usually, in outdoor navigation, exploring unstructured environments is based on or is functional to map making procedures. This paper deals with the problem of representing and updating maps from height field measurements. A technique for dynamic updating maps, in the presence of bounded uncertainties on the height field is presented. The technique is based on the set membership estimation theory, and allows for adaptive refinement of the environment description.

1 Introduction

In outdoor robot navigation, maps are useful for many purposes: localization, e.g. by means of landmark identification and matching [13], path planning and autonomous navigation [9, 5]. Several different approaches have been introduced for describing unknown environments, depending on available sensors, terrain characteristics, etc. [6, 3].
In the exploration of uneven terrain regions, it is common practice to acquire images of the scene and then construct elevation maps of the region. Elevation maps are usually represented through highly structured surfaces [4] which allow to reduce the complexity of the map, and therefore the processing time, which is a mandatory requirement in real time applications. A successful technique for the approximation of elevation maps is the Delaunay triangulation, which is a standard tool in computational geometry [2, 11].
This paper deals with representing and dynamic updating of elevation maps in mobile robots autonomous navigation. While navigating, the robot must update the representation of the surrounding height field. This includes several tasks: removing from the map regions that are not interesting for navigation, including new terrain portions in the map and update the information concerning common areas, exploiting measurements from new data.
Since both sensor measurements and robot motion estimates are affected by errors, map updating should explicitly account for the presence of uncertainty. In this paper, we apply the recently developed set membership estimation theory [10, 8, 7] to the problem of map updating in the presence of bounded errors. An uncertain interval is associated to each point of the elevation map and the uncertainty level is used to adaptively refine the description of the environment.

2 From range images to terrain maps

The exploration of outdoor environments is usually performed through mobile robots equipped with sensors providing *range images*, which are images where the intensity of each pixel is proportional to the distance of the point depicted. Beyond technological motivations, this choice is motivated by the fact that it is easy to retrieve 3D-information from range images. In particular, terrain elevation maps commonly used in navigation planning can be efficiently constructed from range images data.
In the following, a standard technique for the construction of elevation maps from range images is briefly outlined. Let α_h, α_v denote the horizontal and vertical scan angles of the sensor generating the range image and let Δ_α be the sensor angle resolution. Consider a cartesian reference frame $< O >$ fixed at the mobile robot with the range sensor placed at height l. Each measurement provided by the range image is taken along the straight line defined by

$$\begin{cases} x = y \tan(\Gamma_h + i\Delta_\alpha) \\ z = l + y \tan(\Gamma_v + j\Delta_\alpha) \end{cases} \quad (1)$$

where (i,j), s.t. $-\frac{\alpha_h}{2\Delta_\alpha} \leq i \leq \frac{\alpha_h}{2\Delta_\alpha}; -\frac{\alpha_v}{2\Delta_\alpha} \leq j \leq \frac{\alpha_v}{2\Delta_\alpha}$, are the coordinates of the considered point in the range image (referred to the center of the image) and Γ_v (Γ_h) is the initial vertical (horizontal) orientation of the rangefinder.
The distance measured by the sensor, can be expressed in the rectangular coordinates as

$$d(x,y,z) = \sqrt{x^2 + y^2 + (z-l)^2}. \quad (2)$$

Solving (1) and (2) for a known distance d, provides the coordinates of the terrain element (x,y,z) corresponding to any pixel of the image, thus obtaining an

unevenly spaced height field

$$z = h(x, y). \tag{3}$$

In our context the height field (3) represents the measurement equation used to update navigation maps. The finite set of points (x, y), where the measurement equation (3) is defined will be denoted by H.

The environment representation obtained in this way may be inefficient in terms of memory space requirements and computational burden. Since we are interested in mobile robot applications, the minimization of mobile processing power and memory is of paramount importance. Moreover, using height fields, uneven and flat zones are described with almost the same density of points, thus leading alternatively to poor or redundant descriptions.

A possible approach for reducing complexity and convert the discrete representation of the height field into a continuous one is to use the so called *triangulated irregular networks* [4].

The rendering of an height field $h(x, y)$ can be easily obtained by means of triangular meshes. We introduce a reconstruction operator $\mathcal{L}$ mapping a function $h(x, y)$, defined over a discrete set of points H, to a function $\mathcal{L}_H(x, y)$ defined at every point of $\hat{H}$, the convex hull of H. This is accomplished by building a triangulation (i.e. a planar interpolation of each triple of nearest points in h), and using this continuous surface to describe points where $h(x, y)$ is not defined. Note that it is possible to build an approximation of $h(x, y)$ by using an irregular subset $S \subset H$. in this case the surface will be denoted by $z = \mathcal{L}_S(x, y)$ and will be called Triangulated Irregular Network (TIN).

Our goal here is to find the smallest subset S which allows to approximate h for a given accuracy level. This leads one to use triangulation methods that employ *refinement* strategies: we start with a very small subset S_0 (see Fig. 1) and iteratively add new points to the set S until some predefined accuracy threshold is achieved. One of the more efficient and numerically stable algo-

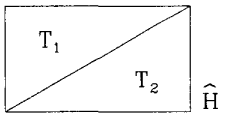

Figure 1: Case of rectangular $\hat{H}$. The height field domain is divided in triangles T_1 and T_2 (subset S_0).

rithms providing a solution to this problem is the *Delaunay triangulation* [2, 11], which uses only the (x, y) projection of the height field. The procedure is specifically designed to maximize the minimum angle of all triangles, thus reducing the occurrence of thin triangles (slivers). Once the accuracy level Δh_T is assigned, the interpolation algorithm starting from a simple triangulation, see Fig. 1, proceeds along the following steps:

Triangulation algorithm

(1) Analyze each triangle T_i: for each point $(x, y) \in T_i \cap H$ evaluate the difference

$$ERR(x, y) = |h(x, y) - \mathcal{L}_S(x, y)|. \tag{4}$$

Find the point $(\bar{x}, \bar{y}) \in T_i \cap H$ which maximizes (4) and, if $ERR(x, y) > \Delta h_T$, add it to a list L of points to be inserted into the triangulation.

(2) When all the triangles have been scanned, choose from L the candidate $(\tilde{x}, \tilde{y})$ that maximizes (4), insert it in the triangulation, using the *incremental Delaunay* method (see [4, 12] for details) and update the list L. Apply the aforementioned analysis (step 1) to all the new triangles, thus generated.

(3) If the list L is not empty, go to step 2.

Note that the test on local error, eq. (4), is very simple from the computational burden point of view, thus satisfying the need for economy of resources.

The algorithm has two inputs: the given accuracy Δh_T and the discrete height field h. The output of the algorithm is the TIN: the set of points S, included in H, defining the triangulated approximation $\mathcal{L}_S(x, y)$ over $\hat{H}$ and such that it satisfies

$$|h(x, y) - \mathcal{L}_S(x, y)| \leq \Delta h_T \quad \forall (x, y) \in H. \tag{5}$$

It is worth noting that more accurate information on the interpolation is gained by storing the worst case interpolation error ${}^i\Delta h_T$ associated with each triangle T_i in S .

3 Maps with uncertainties

During exploration of an unknown outdoor environment, the mobile robot takes different measurements of the surrounding terrain. These views will usually share some information, but each provides some new data, that can be used to improve the construction of the map itself. Assume that the height field domain at sampling time $k + 1$, denoted by $H(k + 1)$, shares a nonempty fraction of the terrain data with the previous domain $H(k)$, see Fig. 2.

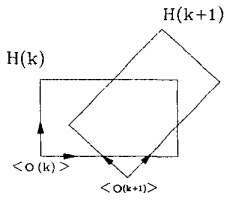

Figure 2: Two height fields domain at different sampling times sharing a non empty area.

In an ideal framework, where both sensor and process noises are negligible, we can assume that the height field provides exact samples of the terrain heights, and that

the robot motion is exactly known at each time instant. This means that the link between the points belonging to both $H(k)$ and $H(k+1)$ can be expressed through the following change of coordinates

$$\begin{cases} \begin{bmatrix} x_i(k+1) \\ y_i(k+1) \end{bmatrix} = R(\theta(k)) \begin{bmatrix} (x_i(k) - x_T(k)) \\ (y_i(k) - y_T(k)) \end{bmatrix} \\ z_i(k+1) = z_i(k) - z_T(k) \end{cases} \quad (6)$$

where $(x_i(k), y_i(k), z_i(k))$ are the coordinates of the i-th point of the map at time k in the current reference frame $< O(k) >$, $(x_T(k), y_T(k), z_T(k))$ and $\theta(k)$ represent the nominal translational and angular displacements covered by the mobile robot in the sampling period, and $R(\theta(k))$ represents a rotation of $\theta(k)$ around the z-axis. Note that in (6) it has been assumed that the i-th point belongs to both grids $H(k)$ and $H(k+1)$.

In a real framework, all the sensor measurements are affected by errors and the robot motion model is also affected by uncertainties. Specifically, rangefinders introduce errors both on distance and direction measurements (due to limited precision and resolution). Moreover, robot localization procedures are affected by errors, both in the case of absolute position measurements (using beacons of known position, or devices such as GPS) and in the case of relative measurements (using odometric integration on wheels encoders). These errors affect the height fields and the map updating process.

With reference to mobile robot kinematics, let us distinguish between relative (odometric) and absolute localization. In the case of odometric measurements with altimetric corrections, mobile robot localization is based on the measurement of the translational and angular commanded displacements which are uncertain:

$$\begin{aligned} &(x_T(k), y_T(k), z_T(k)) = \\ &\quad (\hat{x}_T(k), \hat{y}_T(k), \hat{z}_T(k)) + (e_x(k), e_y(k), e_z(k)), \\ &\theta(k) = \hat{\theta}(k) + e_\theta(k). \end{aligned} \quad (7)$$

Here $(\hat{x}_T(k), \hat{y}_T(k), \hat{z}_T(k))$ and $\hat{\theta}(k)$ represent the nominal (measured) translational and angular motions, while $(e_x(k), e_y(k), e_z(k))$ and $e_\theta(k)$ their relative uncertainties. Then, mobile robot kinematics with odometric uncertainties is modeled by substituting (7) into (6). The prediction of the i-th map point position at time $k+1$, given measurements up to time k, is:

$$\begin{cases} x_i(k+1|k) = f_x(x_i(k), y_i(k), \hat{x}_T(k), \hat{y}_T(k), \hat{\theta}(k)) \\ y_i(k+1|k) = f_y(x_i(k), y_i(k), \hat{x}_T(k), \hat{y}_T(k), \hat{\theta}(k)) \\ z_i(k+1|k) = z_i(k) - \hat{z}_T(k) \end{cases} \quad (8)$$

being f_x, f_y the nonlinear functions in (6). Eq.(8) can be rewritten as

$$\begin{cases} x_i(k+1) = x_i(k+1|k) + \bar{\nu}_i(k) \\ y_i(k+1) = y_i(k+1|k) + \bar{\rho}_i(k) \\ z_i(k+1) = z_i(k+1|k) + \bar{\mu}_i(k) \end{cases} \quad (9)$$

where $\bar{\nu}_i(k)$,$\bar{\rho}_i(k)$ and $\bar{\mu}_i(k)$ account for errors due to uncertainties in (7).

Absolute localization procedures are not affected by odometric uncertainties and do not depend on uncertain kinematics (6)-(7). Absolute localization measurements $(\hat{x}_i(k+1), \hat{y}_i(k+1), \hat{z}_i(k+1))$ provide an estimate of the robot position according to

$$\begin{cases} x_i(k+1) = \hat{x}_i(k+1) + \tilde{\nu}_i(k+1) \\ y_i(k+1) = \hat{y}_i(k+1) + \tilde{\rho}_i(k+1) \\ z_i(k+1) = \hat{z}_i(k+1) + \tilde{\mu}_i(k+1) \end{cases} \quad (10)$$

where $\tilde{\nu}_i(k+1)$, $\tilde{\rho}_i(k+1)$ and $\tilde{\mu}_i(k+1)$ represent uncertainties affecting landmark-based measurements.

Finally, as far as the height field is concerned, uncertainties affecting sensor measurements $\hat{h}_i(x_i(k), y_i(k))$ are modeled by

$$z_i(k) = \hat{h}(x_i(k), y_i(k)) + e_i(k) \quad (11)$$

where $e_i(k)$ accounts for errors on the height field (3).

4 Representation of map uncertainty

Map representation must take into account errors affecting both robot position localization and height field measurements. Clearly, a central role is played by the a priori assumptions on these error terms. In this paper, a set membership description of uncertainty is adopted. Consider for example the measurement equation (11) and assume that the error $e_i(k)$ depends on the distance d_i, see eq. (2), of the terrain element. In fact, it is well known that accuracy of rangefinders measurements is strongly related to the distance of the object from the sensor. In this paper the error term e_i is assumed to be unknown-but-bounded (UBB) in the ℓ_∞ norm:

$$|e_i(k)| \leq \varepsilon |d_i(k)| = \varepsilon_i(k) \qquad \forall k \quad (12)$$

where ε is a known positive scalar depending on the precision and resolution of the height sensor. Similar assumptions can be made on the errors terms in equation (8) and (9).

An important consequence of the above assumptions is that an uncertainty interval can be associated to each point of the height field domain. This means that the *uncertain field*, which will be denoted by $\tilde{h}$, is a function that maps the point $(x_i(k), y_i(k))$ to an interval $[\underline{h}_i(k|k), \overline{h}_i(k|k)]$ where $\underline{h}_i(k|k)$ ($\overline{h}_i(k|k)$) is the lower (upper) bound for the height z_i. Such interval

$$z_i(k) \in \tilde{h}(x_i(k), y_i(k)) = \mathcal{I}\{\underline{h}_i(k|k), \overline{h}_i(k|k)\} \quad (13)$$

can be also expressed as a function of $\hat{h}(k|k) = \frac{\underline{h}_i(k|k) + \overline{h}_i(k|k)}{2}$ and $\Delta h_i(k|k) = \frac{\overline{h}_i(k|k) - \underline{h}_i(k|k)}{2}$ which are respectively the center and the semilength of the uncertainty interval.

To obtain a continuous representation of uncertain height fields, which is efficient in terms of memory space requirements and computational burden, we propose to

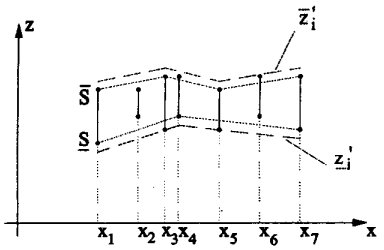

Figure 3: Hard bounds computed from triangulations: $\underline{z}_i' = \mathcal{L}_{\underline{S}}(x_i, y_i) - \Delta h_T(\underline{S})$ is the lower bound and $\bar{z}_i' = \mathcal{L}_{\bar{S}}(x_i, y_i) + \Delta h_T(\bar{S})$ is the new upper bound for the uncertain height field.

use a double triangulation. The first one, $\underline{S}$, renders the lower bounds $\underline{h}_i$, by means of triangular meshes, while the second, $\bar{S}$, approximates the upper bounds $\bar{h}_i$. Both are evaluated on the domain $H(k)$ of the uncertain height field at time k.

Triangulations $\mathcal{L}_{\underline{S}}(x, y)$ and $\mathcal{L}_{\bar{S}}(x, y)$ are evaluated according to the Delaunay technique where the height field is replaced with the lower bound field $\underline{h}(x_i, y_i)$ and the upper bound field $\bar{h}(x_i, y_i)$, respectively.

The proposed double triangulation of the uncertain field allows to characterize height bounds in an efficient way. For any $(x_i, y_i) \in \hat{H}(k)$ the guaranteed error bound on z_i is given by

$$z_i \in h_T'(x_i(k), y_i(k)) = \mathcal{I}\{\underline{z}_i'(k|k), \bar{z}_i'(k|k)\}, \qquad (14)$$

where lower and upper margins are computed directly from triangulations $\mathcal{L}_{\underline{S}}$ and $\mathcal{L}_{\bar{S}}$ as

$$\begin{cases} \text{if} \quad (x_i, y_i) \in \underline{S} & \text{then} \quad \underline{z}_i' = \mathcal{L}_{\underline{S}}(x_i, y_i) \\ \text{if} \quad (x_i, y_i) \in \bar{S} & \text{then} \quad \bar{z}_i' = \mathcal{L}_{\bar{S}}(x_i, y_i) \\ \text{if} \quad (x_i, y_i) \in \hat{H}/\underline{S} & \text{then} \quad \underline{z}_i' = \mathcal{L}_{\underline{S}}(x_i, y_i) - \Delta h_T(\underline{S}) \\ \text{if} \quad (x_i, y_i) \in \hat{H}/\bar{S} & \text{then} \quad \bar{z}_i' = \mathcal{L}_{\bar{S}}(x_i, y_i) + \Delta h_T(\bar{S}). \end{cases} \qquad (15)$$

Additive errors $\Delta h_T(\underline{S})$ and $\Delta h_T(\bar{S})$ are approximation errors of the two triangulations $\mathcal{L}_{\underline{S}}$ and $\mathcal{L}_{\bar{S}}$ and are introduced by Algorithm 1 running on lower and upper bounds. They represent the pay off for the reduction of the amount of data from H to $\underline{S}$ and $\bar{S}$. In Fig. 3, the upper and lower triangulations are reported for a 2D example. In this framework, an upper bound for the triangulation accuracy for the two meshes is provided such that it is guaranteed that the lower triangular mesh $\mathcal{L}_{\underline{S}}$ does not intersect the upper mesh $\mathcal{L}_{\bar{S}}$. The proof of the following proposition is trivial.

Proposition 1 *According to (13), define*

$$\min_{(x_i,y_i)\in H} \frac{\bar{z}_i - \underline{z}_i}{2} = \overline{\Delta h_T},$$

a sufficient condition for

$$\mathcal{L}_{\underline{S}}(x_i, y_i) < \mathcal{L}_{\bar{S}}(x_i, y_i) \quad \forall (x_i, y_i) \in H$$

is that $\Delta h_T(\underline{S}) < \overline{\Delta h_T}$ *and* $\Delta h_T(\bar{S}) \leq \overline{\Delta h_T}$.

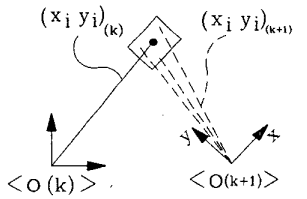

Figure 4: As the robot moves, point $(x_i(k), y_i(k))$ becomes uncertain in the reference frame $< O(k+1) >$.

5 Set membership approach to map updating

This section analyzes how to merge uncertain measurements from different range images sharing a nonempty fraction of the environment (Fig. 2). Let a double triangulation $\mathcal{L}_{S_\Delta}(k|k) = (\mathcal{L}_{\underline{S}}(k|k), \mathcal{L}_{\bar{S}}(k|k))$ be given for points $(x, y) \in \hat{H}(k)$ at the time instant k. At the next time instant, $k+1$, the mobile robot moves to a new position. The problem here is to evaluate the map uncertainty propagation $\mathcal{L}_{S_\Delta}(k+1|k)$ due to robot motion uncertainty (time update).

To explain the main idea underlying the time update procedure, let us focus our attention on a generic point $(x_i(k), y_i(k))$ of $\hat{H}(k)$, Fig. 4. At step $k+1$, the mobile robot has moved to position $< O(k+1) >$ whose relative position with respect to $< O(k) >$ is affected by uncertainty. The mobile robot position uncertainty can be thought of as an uncertainty on vector $(x_i(k+1), y_i(k+1))$ (referred to $< O(K+1) >$) as modeled in the first two equations of (9) and (10) for relative and absolute position measurements.

The most relevant aspect of the proposed set membership filtering procedure consists in embedding the uncertainty on vector $(x_i(k+1), y_i(k+1))$ into the height field $z_i(k+1)$, see eqs. (9) or (10). Let us refer to the relative localization case (9) (analysis for the absolute localization case is analogous). At time $k+1$, an estimation $(x_i(k+1|k), y_i(k+1|k), z_i(k+1|k))$ of a point of the map is provided with relative uncertainties. At the same instant (in the reference frame $< O(k+1) >$) we assume that a map point is given such that the x and y coordinates are known without errors while the z coordinate is uncertain:

$$x_i(k+1) = x_i(k+1|k) \qquad (16)$$

$$y_i(k+1) = y_i(k+1|k) \qquad (17)$$

$$z_i(k+1) = z_i(k+1|k) + \mu_i(k) \qquad (18)$$

where $\mu_i(k) = \bar{\mu}_i(k) + \sigma_i(k)$. That is, uncertainty on mobile robot position has been embedded in a further uncertainty $\sigma_i(k)$ on the z-equation of map points. Uncertainty $\sigma_i(k)$ depends on first order approximations of the surface at point $(x_i(k+1), y_i(k+1))$ and on errors $(\bar{\nu}_i(k), \bar{\rho}_i(k))$. To stress the dependence on the surface unevenness, observe that for flat terrains $\sigma_i(k)$ would be zero.

The error term μ_i is assumed to be unknown-but-bounded (UBB) in the ℓ_∞ norm, i.e.

$$|\mu_i(k)| \leq \gamma_i \quad \forall k \tag{19}$$

where γ_i is a known positive scalar which reflects the a priori knowledge on the estimated robot motion and surface curvature.

Now, it is easy to define the predicted upper and lower triangulations $\mathcal{L}_{S_\Delta}(k+1|k)$, referred to frame $< O(k+1) >$. Upper triangular mesh $\mathcal{L}_{\overline{S}}(k+1|k)$ is defined through vertices $(x_i(k+1), y_i(k+1))$ obtained from eqs. (16)–(17) evaluated at points $(x_i(k), y_i(k)) \in \overline{S}(k|k)$ and computing the z–coordinate as $z_i(k+1|k) + \gamma_i$. Computation of predicted lower triangular mesh $\mathcal{L}_{\underline{S}}(k+1|k)$ is analogous.

The predicted double triangulation of the uncertain field allows to characterize predicted height bounds on the map in an efficient way. For any $(x_i(k+1|k), y_i(k+1|k)) \in \hat{H}(k)$ guaranteed error bounds are given by

$$z_i(k+1|k) \in \mathcal{I}\{\underline{z}'_i(k+1|k), \overline{z}'_i(k+1|k)\} \tag{20}$$

where lower and upper margins are computed from $\mathcal{L}_{\underline{S}}(k+1|k)$ and $\mathcal{L}_{\overline{S}}(k+1|k)$ similarly to eq. (15).

A 2D example of uncertainty map propagation is given in Fig. 5. Uncertainties $\bar{\nu}_i(k)$ on points $x_i(k+1) \in \hat{H}(k+1)$ are embedded in the height uncertainties of points in $\overline{S}(k+1|k)$ and $\underline{S}(k+1|k)$ which exhibit the same cardinality of triangulations $\overline{S}(k|k)$ and $\underline{S}(k|k)$. Note that tighter bounds can be obtained at the cost of computing a new triangular mesh for lower and upper bounds, see $\overline{S}^*(k+1|k)$ in Fig. 5, which in general are characterized by a higher number of vertices.

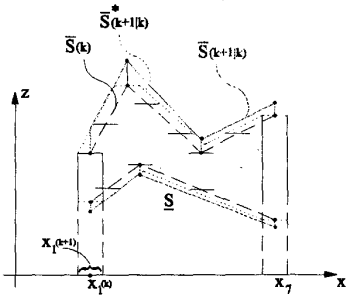

Figure 5: A 2D example of uncertainty map propagation.

The updating map procedure aims at reducing uncertainty affecting a point which belongs both to the map domain $\hat{H}(k)$ and the new grid $H(k+1)$ by exploiting previous triangulations and new measurements provided by the rangefinder.

Once the predicted uncertain triangulation $\mathcal{L}_{S_\Delta}(k+1|k)$ has been computed, one can exploit the new measurements provided by the range image at time $k+1$ in order to improve the map description (measurement update).

In the following, a procedure is described which allows to merge information from predicted triangular meshes $(\mathcal{L}_{\underline{S}(k+1|k)}, \mathcal{L}_{\overline{S}(k+1|k)})$ and the new measurement of the uncertain field over $H(k+1)$.

For any $(x_i(k+1), y_i(k+1)) \in \hat{H}(k) \cap H(k+1)$, the updated interval of the height field $z_i(k+1)$ is computed by intersecting the predicted and measurement uncertainty intervals, given by

$$z_i(k+1) \in \mathcal{I}\{\underline{z}'_i(k+1|k), \overline{z}'_i(k+1|k)\} \bigcap \mathcal{I}\{\hat{h}(k+1) - \varepsilon_i(k+1), \hat{h}(k+1) + \varepsilon_i(k+1)\}$$

where $\hat{h}(k+1)$ is the height measurement in (11).

Finally, for points in $H(k+1)$ which do not belong to $\hat{H}(k)$, one sets

$$z_i(k+1) \in \mathcal{I}\{\hat{h}(k+1) - \varepsilon_i(k+1), \hat{h}(k+1) + \varepsilon_i(k+1)\}.$$

Summing up, the overall algorithm for uncertain map updating can be sketched as follows.

Algorithm

(0) Let $\mathcal{L}_{S_\Delta}(k|k)$ be given at time k.

(1) Propagate errors of the lower and upper bound triangular meshes by computing $\mathcal{L}_{S_\Delta}(k+1|k)$.

(2) Update the uncertainty intervals associated to the height of points in $H(k+1)$ merging information given by predicted meshes at points in $\hat{H}(k) \cap H(k+1)$ and measurements provided by the rangefinder at points $H(k+1)$.

(3) Compute upper and lower triangulations for the resulting uncertain height fields in $H(k+1)$, thus obtaining $\mathcal{L}_{S_\Delta}(k+1|k+1)$.

Uncertainty-based map updating

The uncertainty associated to the points of the map can be exploited in order to improve the quality of the map in the regions where measurements are more accurate. The updating algorithm can be modified in order to have an adaptive goal testing. A possible approach consists in choosing a threshold value for $ERR(x,y)$ in eq. (4), which depends on some measure of the uncertainty affecting the height field in one or more regions. This allows to produce good data approximation (fine triangulation) where the data quality is good, while keeping a rough terrain representation where data is more uncertain.

Since the uncertainty bounds usually change moving on the map, we choose a synthetic measure of quality for any element T of the triangulation, which takes into account the whole uncertainty affecting the points in T. There are basically two different choices:

- Use the maximum uncertainty bound found over a set of points of T;
- Use the mean value of all uncertainties in T.

In both cases, the set of points to include in the analysis may be as small as the vertices of the triangle, or bigger (up to all the points of H included in T).

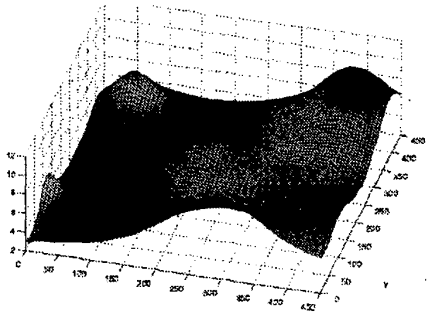

Figure 6: The height field of a synthetic tridimensional environment.

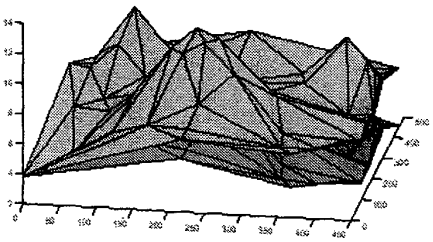

Figure 7: Triangulation of upper and lower bounds bounding the real height field.

6 Simulation results

A synthetic environment is used for simulation purposes. The height field of the environment is reported in Fig. 6. The absolute localization procedure is considered. For the sake of simplicity errors on the mobile robot angle θ are disregarded. The UBB error parameter in (12) is set to $\varepsilon = 0.05$.
Two different sets of measurements are processed. The mobile robot with the rangefinder is initially positioned at the origin. At the second step mobile robot translate by vector $(50, 50, 0)$. Further details can be found in [1]. The resulting bounding triangulation is reported in Fig. 7 where the lower triangulation is that of lower bounds and the upper triangulation is that of upper bounds. In the spirit of the set membership approach, this representation guarantees that the real height field is bounded by the two triangulations.

7 Conclusions

A set mempership filtering procedure is proposed for dynamic updating of uncertain elevation maps. The set membership updating algorithm requires very few calculations and therefore is suitable for potential on–line implementation. Different strategies for the choice of the threshold on $ERR(x, y)$, as a function of the uncertainty level associated to the considered triangle, can be devised. This clearly influences the quality of terrain representations. Comparisons between different heuristics are currently under experimentation. The use of the uncertain elevation maps in landmark-based localization and path planning problems will be the subject of future research. Experiments of the proposed technique on real height fields are in progress.

Acknowledgments

The authors wish to thank the student Annalisa Cavallini of the University of Siena for her support in running simulations.

References

[1] A. Cavallini Polygonal approximation of maps with uncertainties for mobile robot navigation (in italian) *Master Thesis* University of Siena, 1999.

[2] M. Bern, D. Eppstein, and J. R. Gilbert. Provably good mesh generation. *Journal of Computer and System Sciences*, 48(3):384–409, 1994.

[3] S. Betgé-Brezetz, P. Hébert, R. Chatila, and M. Devy. Uncertain map making in natural environments. In *Proc. of the 1996 IEEE Int. Conf. on Robotics and Automation*, pages 1048–1053, Minneapolis, April 1996.

[4] M. Garland and P. S. Heckbert. Fast polygonal approximation of terrain and height fields. Technical Report CMU-CS-TR-95-181, Computer Science Department, Carnegie Mellon University, 1995.

[5] S. Lacroix and R. Chatila. Motion and perception strategies for outdoor mobile robot navigation in unknown environments. In *4th International Symposium on Experimental Robotics*, pages 337–342, Stanford (USA), June 1995.

[6] S. Lacroix, R. Chatila, S. Fleury, M.Herrb, and T. Simeon. Autonomous navigation in outdoor environment: adaptive approach and experiment. In *IEEE International conference on Robotics and Automation*, pages 426–432, San Diego, May 1994.

[7] M. Milanese, J. P. Norton, H. Piet-Lahanier, and E. W. (eds.). *Bounding Approaches to System Identification.* Plenum Press, New York, 1996.

[8] M. Milanese and A. Vicino. Optimal estimation theory for dynamic systems with set membership uncertainty: an overview. *Automatica*, 27(6):997–1009, 1991.

[9] F. Nashashibi, P. Fillatreau, B. Dacre-Wright, and T. Simeon. 3D autonomous navigation in a natural environment. In *IEEE International conference on Robotics and Automation*, pages 433–439, San Diego, May 1994.

[10] J. P. Norton. Identification and application of bounded-parameter models. *Automatica*, 23:497–507, 1987.

[11] J. Ruppert. A Delaunay refinement algorithm for quality 2-dimensional mesh generation. *Journal of Algorithms*, 18(3):548–585, 1995.

[12] J. R. Shewchuk. Triangle: Engineering a 2D quality mesh generator and Delaunay triangulator. In *First Workshop on Applied Computational Geometry*, pages 124–133, Philadelphia, May 1996.

[13] K. T. Sutherland and W. B. Thompson. Localizing in unstructured environments: dealing with the errors. *IEEE Transactions on Robotics and Automation*, 10(6):740–754, 1994.